Lasers Med Sci (2013) 28:203–213
DOI 10.1007/s10103-012-1110-7

ORIGINAL ARTICLE

Histological and SEM analysis of root cementum following irradiation with Er:YAG and CO_2 lasers

Aslam Almehdi · Akira Aoki · Shizuko Ichinose · Yoichi Taniguchi · Katia M. Sasaki · Kenichiro Ejiri · Masanori Sawabe · Chanthoeun Chui · Sayaka Katagiri · Yuichi Izumi

Received: 21 November 2011 / Accepted: 17 April 2012 / Published online: 13 May 2012

Abstract Recently, the Er:YAG and CO_2 lasers have been applied in periodontal therapy. However, the characteristics of laser-irradiated root cementum have not been fully analyzed. The aim of this study was to precisely analyze the alterations of root cementum treated with the Er:YAG and the CO_2 lasers, using non-decalcified thin histological sections. Eleven cementum plates were prepared from extracted human teeth. Pulsed Er:YAG laser contact irradiation was performed in a line at 40 mJ/pulse (14.2 J/cm^2/pulse) and 25 Hz (1.0 W) under water spray. Continuous CO_2 laser irradiation was performed in non-contact mode at 1.0 W, and ultrasonic instrumentation was performed as a control. The treated samples were subjected to stereomicroscopy, scanning electron microscopy (SEM), light microscopy and SEM energy dispersive X-ray spectroscopy (SEM-EDS). The Er:YAG laser-treated cementum showed minimal alteration with a whitish, slightly ablated surface, whereas CO_2 laser treatment resulted in distinct carbonization. SEM analysis revealed characteristic micro-irregularities of the Er:YAG-lased surface and the melted, resolidified appearance surrounded by major and micro-cracks of the CO_2-lased surface. Histological analysis revealed minimal thermal alteration and structural degradation of the Er:YAG laser-irradiated cementum with an affected layer of approximately 20-μm thickness, which partially consisted of two distinct affected layers. The CO_2-lased cementum revealed multiple affected layers showing different structures/staining with approximately 140 μm thickness. Er:YAG laser irradiation used with water cooling resulted in minimal cementum ablation and thermal changes with a characteristic microstructure of the superficial layer. In contrast, CO_2 laser irradiation produced severely affected distinct multiple layers accompanied by melting and carbonization.

Keywords Cementum · Alteration · Microstructure · Er:YAG laser · CO_2 laser · Ultrasonic scaler

A. Almehdi · A. Aoki (✉) · Y. Taniguchi · K. Ejiri · M. Sawabe · C. Chui · S. Katagiri · Y. Izumi
Department of Periodontology,
Graduate School of Medical and Dental Sciences,
Tokyo Medical and Dental University (TMDU),
1-5-45 Yushima, Bunkyo-ku,
Tokyo 113-8549, Japan
e-mail: aoperi@tmd.ac.jp

A. Almehdi · C. Chui · Y. Izumi
Global Center of Excellence (GCOE) Program,
International Research Center for Molecular Science in Tooth and Bone Diseases, Tokyo Medical and Dental University,
Tokyo, Japan

S. Ichinose
Research Center for Medical and Dental Sciences,
Tokyo Medical and Dental University,
Tokyo, Japan

K. M. Sasaki
Department of Dentistry, Brasilia University,
Brasillia, Brazil

Introduction

Periodontitis is a chronic inflammatory and infectious disease that leads to progressive destruction of alveolar bone and teeth loss [1]. It is characterized by gingival inflammation, pocket formation and bone resorption. The primary goal in treatment of periodontal disease is to arrest the inflammation by removal of microbial deposits, resulting in periodontal tissue regeneration [2]. Initial periodontal therapy aims to remove bacterial plaque and calcified

deposits from the diseased root surface and thus restore its biological compatibility.

Conventional mechanical instrumentation is an effective treatment approach for diseased root surfaces [3, 4]. However, complete removal of adherent plaque and calculus is not always achieved by mechanical instruments [3, 5]. Therefore, various innovative treatments including lasers were employed to improve the clinical effectiveness of root debridement [6, 7].

Currently, lasers are considered one of the most promising new technical modalities for periodontal therapy. Conventional laser systems such as the CO_2 and the Nd:YAG lasers were effectively used for soft tissue management [8]; however, these lasers could not be applied on hard tissue. With development of the Er:YAG laser, laser applications were further expanded to hard tissue treatment [9–11]. Since the wavelength (2.94 μm) of the Er:YAG laser is resonant to the water molecule and thereby is well absorbed by water [12], the laser is capable of effectively ablating hard tissues without major thermal side effects [9–11]. The hypothesized mechanism of hard tissue ablation with the Er:YAG laser is the thermo-mechanical effect induced by 'micro-explosion' of water molecules within the hard tissue [6, 9, 10]. Thus, the Er:YAG laser system enables light energy to perform root surface debridement [13, 14]. Several in vitro and in vivo studies have demonstrated that the Er:YAG laser is capable of removing subgingival calculus from the root cementum [15–18]. Unlike mechanical scaling and root planing, the Er:YAG laser scaling of root surfaces has been reported to favorably preserve root cementum [15, 16, 19]. Recently, the Er:YAG laser was applied for debridement of the diseased root surface in non-surgical and surgical periodontal therapy and the clinical effectiveness has been reported [14, 20, 21].

Regarding Er:YAG laser-treated root cementum, previous studies have demonstrated minimal thermal changes and microstructured topography of root cementum following irradiation [6]. The CO_2 laser is also frequently used for gingivectomy around the tooth root; however, inadvertent irradiation on the tooth surface may result in major damage to root cementum/dentin during procedure [8, 22]. However, changes of lased root cementum have not been thoroughly analyzed yet and the existing evidence is not sufficient. Also, the effects of the Er:YAG laser recently available at high pulse rates are unknown.

Therefore, the aim of the present study was to precisely analyze the microstructural alterations of root cementum following irradiation with high-pulse-rate Er:YAG laser and continuous wave CO_2 laser in comparison with that of ultrasonic scaling, using non-decalcified thin sections for histological analysis.

Materials and methods

Sample collection and cementum plate preparation

This study used intact human molars and premolars. The teeth had been extracted due to pericoronitis or for orthodontic treatment from patients who attended the Dental Hospital, Tokyo Medical and Dental University as well as a private dental clinic, after obtaining informed consent. After extraction, the teeth were stored in saline solution at −20 °C.

Prior to the experiment, the frozen teeth were thawed and the remaining soft tissues were removed by approximately 10 min of ultrasonication in 5 % sodium hypochlorite solution. Then, approximately 40 teeth with suitable root size and shape were selected, and a cementum plate of dimension 4×4×1 mm was prepared from each root. Then, the plates with a relatively flat and large surface and without any damage or pits were carefully selected. Consequently, a total of 11 cementum plates were employed for the final experiment. All plates were stored at 4 °C until the experiment. The protocol of the present study was approved by the Ethics Committee of the Faculty of Dentistry, TMDU (no. 550).

Experimental design and procedure

Each cementum surface was divided into longitudinal thirds. The first one-third was treated by ultrasonic instrumentation, the middle one-third with Er:YAG laser irradiation, and the last one-third by CO_2 laser.

Ultrasonic instrumentation

A piezoelectric type ultrasonic scaler (Solfy™, J. Morita. Mfg. Corp., Kyoto, Japan) and its universal tip with a sharp point were used. Instrumentation with water spray was performed in a line for 2 s, maintaining the tip in contact obliquely to the surface at an angle of 30° with moderate pressure. The power setting used was 4, which is the standard for clinical scaling within the 2–6 power range.

Er:YAG laser irradiation

An Er:YAG laser apparatus with a wavelength of 2,940 nm (Erwin Adverl™, J Morita Mfg. Corp.; pulse width 250 μs and hollow wave-guide delivery) and an brand-new, 80° curved contact tip with a diameter of 600 μm (no.C600F) was used. Pulsed laser irradiation with water spray was performed in a line for 2 s with the tip obliquely in contact to the surface at an angle of 30°. An energy output of 40 mJ/pulse (panel setting 70 mJ/pulse, energy density 14.2 J/cm^2/pulse) and pulse repetition rate of 25 Hz (1 W) were used, which is suitable for root debridement with this laser apparatus. The energy output/density was determined based on

the protocol applied in our previous study [16] and the energy output was measured using a power meter (Field Master™; Coherent Co., Santa Clara, CA, USA).

CO_2 laser irradiation

A CO_2 laser with a wavelength output of 10,600 nm (Opelaser-03 S™; Yoshida Co. Ltd, Tokyo, Japan) was employed. Continuous irradiation was performed in a line for 2 s in non-contact, focused mode (beam diameter: 400 μm) at 30° to the cementum surface. The power was 1.0 W, which was equal to that of Er:YAG laser irradiation.

Stereo-microscopy

Immediately after treatment, all the specimens were inspected and photographed using a stereomicroscope.

Scanning electron microscopy (SEM)

Four out of the 11 specimens were randomly selected for SEM. They were fixed in 2.5 % glutaraldehyde for 2 h and washed overnight in 0.1 M phosphate-buffered saline at 4 °C. Then, the specimens were post-fixed with 1 % osmium tetraoxide for 2 h at 4 °C and dehydrated in graded ethanol solutions. After washing with 3 methyl butyl acetate and dried to the critical point, the specimens were coated with platinum. The surface was observed under a scanning electron microscope (S-4500 SEM; Hitachi Ltd., Hitachinaka, Japan).

Light microscopy

The remaining seven specimens were fixed in glutaraldehyde, post-fixed with osmium tetraoxide, dehydrated, washed with propylene oxide, and embedded in epoxy resin. After polymerization, each specimen was divided into two parts and one half of each was used. Cross-sections of 1-μm thickness at the sites near the middle of the original linear treatment were prepared using a glass knife mounted on an ultra-microtome (Reichert Ultracut S, Leica, Austria). The sections were stained with 0.1 % toluidine blue and observed under light microscope. Width of the treated region and depth of ablation of each treated site were measured for each section.

SEM energy dispersive X-ray spectroscopy (SEM-EDS)

The remaining halves of the seven specimens examined by light microscopy were employed. One cross-sectional surface near the middle of the original linear treatment for each specimen was analyzed. Each surface was polished with a glass knife. The specimens were mounted and sputter-coated with osmium plasma. For each surface, one site around the middle of each treated region, avoiding the artifacts such as major cracks and defects, was subjected to line-scan analysis using an energy dispersive X-ray micro-analyzer device (EMAX-7000; Horiba Ltd., Kyoto, Japan) attached to the SEM with an acceleration voltage of 20 kV for 1,200 s. In the analysis of Ca, P and O, the relative intensity of the characteristic X-rays of Ca $K\alpha_1$, P $K\alpha_1$ and O $K\alpha_1$ were determined, respectively. The analyzed line extended from the border of the treated surface to a deep, intact site. According to the results of pilot experiments, the depth of the line-scan analysis was determined as approximately 30 μm for both the ultrasonic scaler and the Er:YAG laser and approximately 200 μm (×3,000 in SEM) for the CO_2 laser (×400 in SEM) in order to reach the intact site.

Determination of the affected layer

Histological analysis

For each section, three distinct points were selected at regular intervals on the surface of the treated region and the thickness of the stained layer was determined. The three original data points were averaged and the average was denominated as the representative value of each treatment for each specimen. Then, the average of those representative values of the seven specimens of each treatment group was calculated as the representative value of each group.

SEM-EDS analysis

After measurement of EDS, the thickness of the affected layer based on the change of Ca and P amounts as well as the change in the difference of Ca and P amounts were determined in all the profiles and the average was calculated for each treatment. The average was denominated as the representative value of each treatment.

Statistical analysis

Kruskal–Wallis test was applied to evaluate the thickness of the affected layer in the three different treatment methods for histological and SEM-EDS analysis. Games–Howell test as a post-hoc test was performed to detect differences between two specific treatments. Unpaired *t*-test was employed to compare the thickness of affected layer between histological and SEM-EDS assessments for each treatment method. The level of significance was set at $p < 0.05$. A software program (SPSS® version 19.0; SPSS Inc., Chicago, IL, USA) was used.

Results

Stereo-microscopy

Steromicroscopic observation revealed that the ultrasonic scaler-treated cementum surface had a relatively smooth and glossy surface with small defects created by ultrasonic vibration of the tip. The line made by Er:YAG laser irradiation exhibited a slightly rugged, whitish appearance with precise margins made of a series of round spots due to the pulsed irradiation. The CO_2 laser treatment produced a distinct black carbonized line accompanied with areas presenting a whitish product over the carbonization (Fig. 1).

SEM

At low magnification (×100), the non-treated cementum had a smooth surface (Fig. 2a) and the ultrasonically treated cementum surface exhibited a shallow groove with the polished appearance of original cementum and visible instrumentation marks (Fig. 2b). The Er:YAG laser-treated cementum showed a fine micro-rough surface with no smear layer (Fig. 2c). CO_2 laser-treated cementum presented a melted and resolidified, concaved surface and partly rugged defect with major cracks (Fig. 2d).

At moderate (×500) and high (×3,000) magnifications, the non-treated intact cementum showed numerous round-shaped structures with some surrounding space which was probably created by shrinkage of collagen fiber bundles

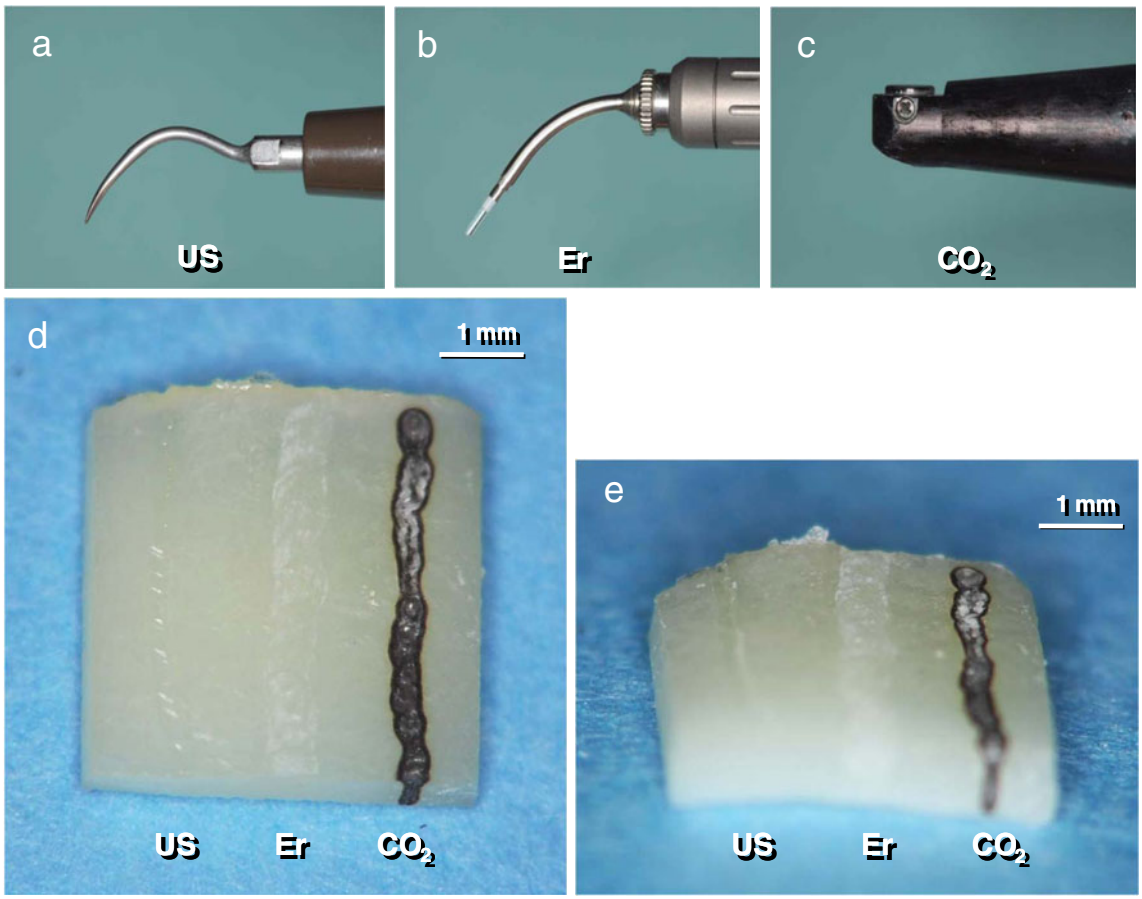

Fig. 1 Ultrasonic scaler, Er:YAG laser and CO_2 laser, and each treated line on root cementum. Ultrasonic scaler tip with a sharp point (**a**), Er:YAG laser contact tip with 600 μm in diameter (**b**) and CO_2 laser non-contact handpiece (**c**). The ultrasonic treatment was performed with water spray at a power setting of 4 with moderate pressure for 2 s. The Er:YAG laser treatment was performed at 40 mJ/pulse (energy density: 14.2 J/cm^2/pulse) and 25 HZ (1 W) with water spray for 2 s. The CO_2 laser treatment was performed at 1.0 W without coolant in a non-contact focused mode for 2 s. Front view (**d**) and transversal view (**e**) of cementum plate after treatment are presented. The line treated with ultrasonic scaler showed a relatively smooth and glossy surface with small defects created by the ultrasonic vibration of the tip. The line made by Er:YAG laser irradiation exhibited a slightly rugged, whitish appearance with precise edges made of a series of round spots due to the pulsed irradiation. The CO_2 laser treatment produced a distinct black carbonized line accompanied with areas presenting a whitish product over the carbonization. *US* ultrasonic scaler, *Er* Er:YAG laser, *CO_2* CO_2 laser

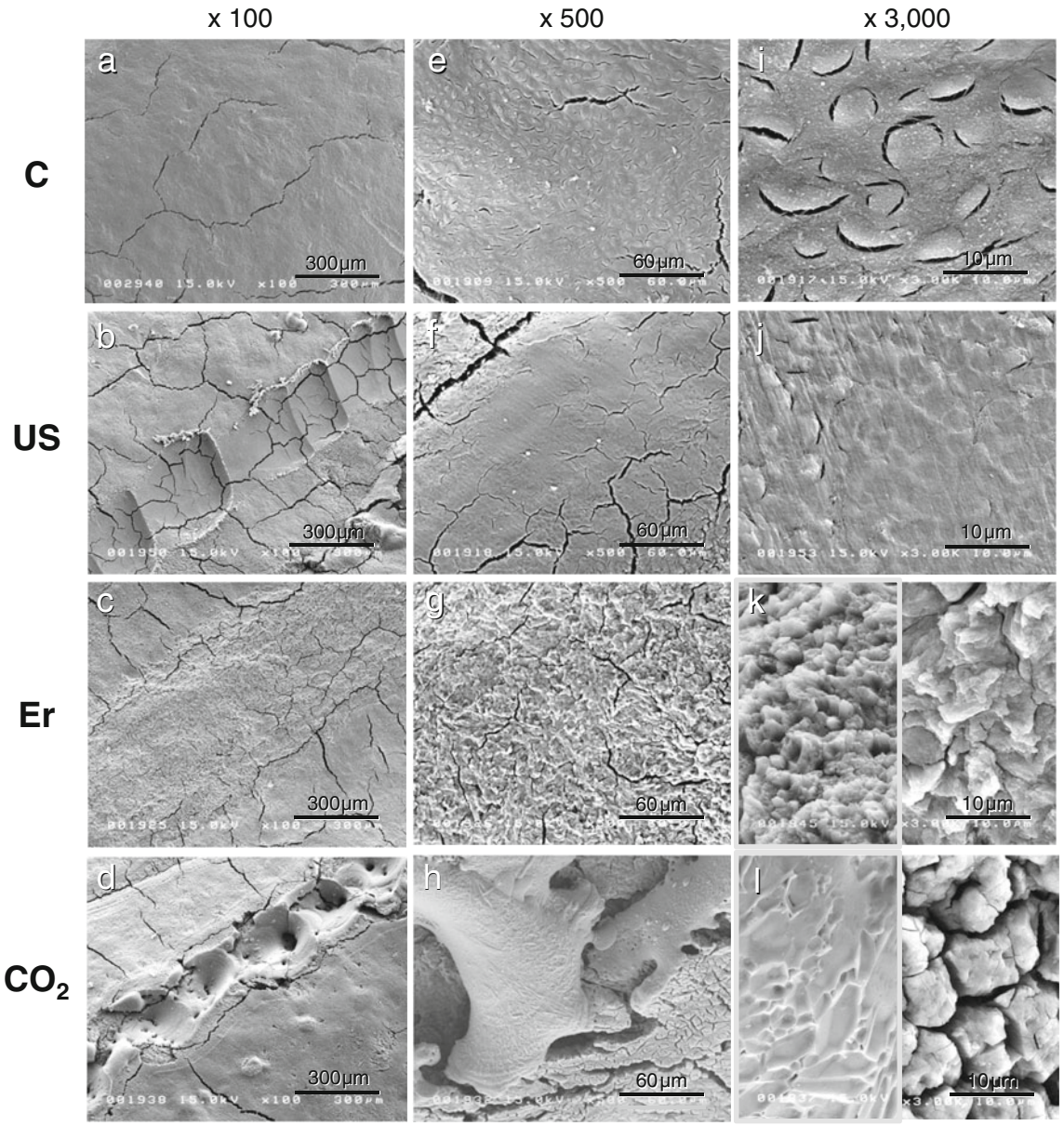

Fig. 2 Scanning electron micrographs of treated root cementum. At low magnification (×100), the non-treated cementum shows smooth surface (**a**) and the ultrasonically treated cementum surface exhibited a shallow groove with the polished appearance of original cementum and visible instrumentation marks (**b**). The Er:YAG laser-treated cementum showed a micro-rough surface in a fine pattern (**c**). CO_2 laser-treated root cementum presented a melted and resolidified, concaved surface and partly rugged defect (**d**). At moderate (×500) and high (×3,000) magnifications, the non-treated intact cementum surface showed numerous round shaped structures with some surrounding space (**e**, **i**). The ultrasonically treated cementum presented a smooth surface (**f**) with a polished appearance of the round shaped structures (**j**). The Er:YAG-lased cementum showed a characteristic grass-like or flaky appearance with homogeneously distributed pointed or round projections (**g**, **k**). The CO_2 laser treated-root cementum presented melted and resolidified structures as well as shrunken structures with numerous major and microcracks. (**h**, **l**). *C* non-treated control cementum, *US* ultrasonic scaler, *Er* Er:YAG laser, *CO_2* CO_2 laser

(Sharpey's fibers) during the drying step of specimen preparation (Fig. 2e,i). The ultrasonically treated cementum presented a smooth surface with a polished appearance of the round-shaped structures (Fig. 2f,j). The Er:YAG-lased cementum showed a characteristic grass-like or flaky appearance with homogeneously distributed pointed or round projections (Fig. 2g,k). The CO_2 laser treated-root cementum presented melted and resolidified structures surrounded by shrunken structures with numerous major and micro-cracks (Fig. 2h,i).

Light microscopy

The non-treated cementum showed a smooth surface with minimal staining (Fig. 3a,b). The ultrasonically

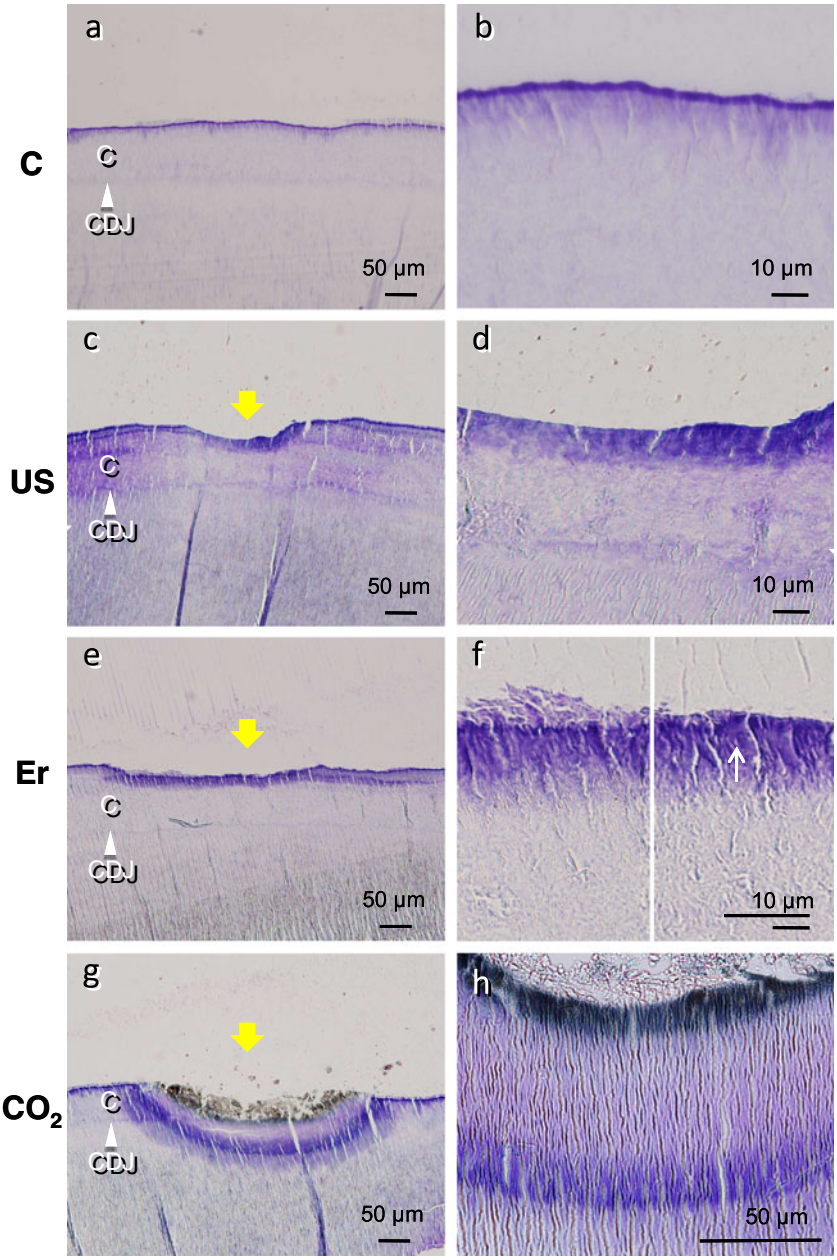

Fig. 3 Photomicrographs of non-decalcified thin histological sections. Non-treated cementum surfaces showed a smooth surface with minimal staining (**a**, **b**). Ultrasonically instrumented cementum surfaces showed a shallow groove with a thin, darkly stained layer and minimal ablation (**c**). At a high magnification, the treated site exhibited a smooth surface with dark staining. (**d**). The Er:YAG laser-treated cementum presented a shallow and wide groove with an irregular border and a thin, darkly stained surface layer. Partly a specific, serrated irregular surface was observed (**e**). At high magnification, the specific irregular surface consisted of two different layers: a lightly stained less dense superficial layer with numerous microcracks, and a darkly stained deep layer (**f**, *left*). In the CO_2 laser-treated root, extensive thermal changes were clearly visible. The irradiated site presented a dome-shaped large stained area with different structures or stained layers (**g**). At a high magnification, the stained area was divided into approximately five different layers: completely denatured transparent or light-brown colored layer, carbonized black layer, and some differently stained layers from the surface to deeper sites (**h**). In all the pictures, microcracks seen in the same direction were artifacts produced during sectioning of non-decalcified specimens. *C* non-treated control cementum, *US* ultrasonic scaler, *Er* Er:YAG laser, *CO_2* CO_2 laser, *C* cementum layer, *CDJ* cemento-dentinal junction. *Arrows* indicate the site of each treatment on the cementum surface

instrumented surfaces showed a shallow groove with a thin, darkly stained layer. Cementum ablation was generally minimal with a width of approximately 253.1± 92.7 μm and depth of 33.0±12.4 μm (n=7, mean±SD) (Fig. 3c). At high magnification, the treated site exhibited a smooth surface with dark staining. The ablation/affected layer was within cementum in all the specimens (Fig. 3d). Microcracks seen in the same

direction were artifacts produced during sectioning of non-decalcified specimens.

The Er:YAG laser-treated cementum presented a shallow and wide groove sized 562.7±56.6 μm in width and 51.6± 25.8 μm in depth (n=7, mean ± SD). The lased surface generally showed an irregular border with a thin, darkly stained layer. Partly a specific, serrated irregular surface was observed (Fig. 3e). At high magnification, the specific irregular surface consisted of two different layers: a lightly stained superficial layer and a darkly stained deep layer. The superficial layer revealed thermal alteration as well as high structural degradation including numerous microfissures and microcracks occasionally resulting in microfragmentation. The deep layer exhibited mainly thermal changes (Fig. 3f). The ablation/affected layer was within cementum except in one specimen.

In the CO_2 laser-treated root, extensive thermal changes were clearly visible. The irradiated site presented a dome-shaped large stained area with different structures or multiple stained layers of width 423.1±90.9 μm and depth 181.8±24.6 μm, including a superficial defect of depth 47.7±19.8 μm (n=7, mean ± SD) (Fig. 3g). At high magnification, the stained area could be divided into approximately five different layers: a completely denatured transparent or light-brown colored layer, a carbonized black layer, and some differently stained layers from the surface to deep sites (Fig. 3h). The ablation/affected layer reached dentin in all of the specimens.

SEM-EDS

The height of the line graph shows the X-ray strength, which corresponds to the relative quantity of each element. In normal cementum and dentin, the Ca level was always higher than P level; however, in the thermally affected tissue except for the superficial layer of CO_2-lased tissue, their levels almost coincided or the difference between both levels became much smaller, compared to that of the deeper unaffected tissue.

In the EDS analysis of the non-treated control cementum, from the deep site to the site beneath the surface, both Ca and P levels were almost constant and Ca was always higher than P. At the site close to the surface, both elements rapidly decreased towards the treated surface showing the same value (Fig. 4a). The ultrasonic treated specimens basically showed almost the same pattern as that of the non-treated control. However, the reduction of both elements on the surface was more rapid and the superficial layer showing same levels of Ca and P was thicker than that of the control (Fig. 4b).

In the Er:YAG laser treated-root cementum, both Ca and P levels gradually decreased towards the surface from a site deeper than in ultrasonic treatment, and the Ca and P levels almost coincided with each other while decreasing. In the superficial layer, both the Ca and P as well as O amounts slightly or moderately increased in most of the specimens, and then rapidly decreased towards the surface (Fig. 4c).

In CO_2 laser treatment, Ca and P gradually decreased or increased at an equal level from a site much deeper than that in Er:YAG laser treatment, and a marked increase of Ca and P, a higher amount of Ca than P, and a slight to moderate increase of O level were noted at the superficial layer (Fig. 4d).

Determination of the affected layer

In the histological analysis, the thickness of the affected layer of the treated surface determined by zone of staining was 12.9±5.4 μm (mean ± SD, n=7, range: 6.6–20.0 μm) for the ultrasonic treatment, 21.1±2.4 μm (range: 18.2–25.3 μm) for the Er:YAG laser treatment, and 143.0± 19.7 μm (range: 120.4–166.5 μm) for CO_2 laser treatment (Fig. 5).

In the SEM-EDS analysis, the thickness of the affected layer determined by the change of Ca and P levels as well as the change in the difference of both levels was 7.0±3.3 μm (mean ± SD, n=7, range: 3.4–11.2 μm) for the ultrasonic treatment, 14.7±2.3 μm (range: 12.7–16.1 μm) for the Er:YAG laser treatment, and 137.7±23.8 μm (range: 103.2–165.9 μm) for CO_2 laser treatment (Fig. 5).

The affected layer produced by CO_2 laser (CO_2) was markedly thicker than those of the Er:YAG laser (Er) and the ultrasonic scaler (US). Statistically, the thickness of affected layer differed significantly among the three different treatments in each assessment (p<0.01). The thickness of the affected layer was significantly different between any two treatments in the histological analysis (US vs. Er: p< 0.05; US vs. CO_2, Er vs. CO_2: p<0.01) and in the SEM-EDS analysis (US vs. Er, US vs. CO_2, Er vs. CO_2: p<0.01). Comparing the histological and EDS assessments, the thickness in histological analysis was significantly higher than that in SEM-EDS with the Er:YAG laser (p<0.05) and with the US treatment (p<0.05).

Discussion

In the present study, the non-decalcified thin histological sections employed could preserve the original surface microstructure of the Er:YAG or CO_2 laser-treated cementum, and this method revealed alterations of the lased cementum surfaces precisely.

Regarding the Er:YAG laser, production of a thin deeply stained zone on the lased cementum has been previously observed; however, the presence of two layers in the altered cementum was not clearly indicated in the microphotograph of decalcified sections [16]. In the present study, the presence of two distinct layers with microstructural differences was

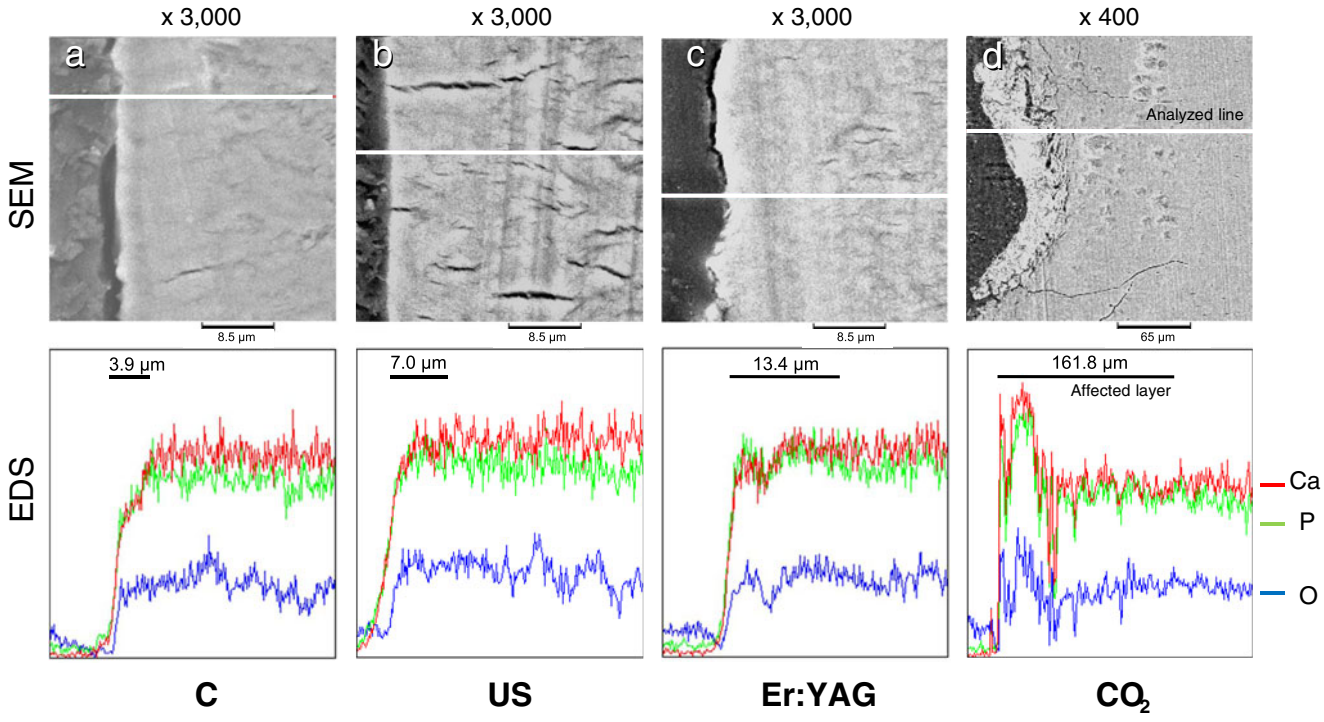

Increase of elements in the superficial layer

sample No.	1	2	3	4	5	6	7	1	2	3	4	5	6	7	1	2	3	4	5	6	7	1	2	3	4	5	6	7
Ca, P	-	-	-	-	-	-	+	-	-	-	-	-	-	-	+	+	-	+	+	+	+	++	++	++	++	++	++	++
O	-	-	-	-	-	-	-	-	-	-	+	-	-	-	+	++	+	+	++	+	-	++	++	++	+	+	+	+

Fig. 4 Scanning electron microscopy-energy dispersive X-ray spectroscopy (*SEM-EDS*): line micro-analysis of treated-root cementum. The height of the line graph shows the X-ray strength, which corresponds to the relative quantity of each element. In the non-treated control and US-treated cementum, from a deep site to the site beneath the surface, both Ca and P levels were almost constant and Ca was always higher than P. Then, at the site close to the surface both elements rapidly decreased towards the treated surface (**a**, **b**). In the US-treated cementum, the reduction of both elements on the surface was more rapid and the superficial layer showing same levels of Ca and P was thicker than that of the non-treated control (**b**). The Er:YAG laser treated-root cementum showed that both Ca and P levels gradually decreased towards the surface from a site deeper than that in ultrasonic treatment, and the Ca and P levels almost coincided with each other while decreasing. In the superficial layer, both Ca and P as well as O amounts slightly or moderately increased in most of the specimens, and then rapidly decreased towards the surface (**c**). In CO_2 laser treatment, Ca and P gradually decreased or increased at equal levels from a very deep site and a marked increase of Ca and P and slight to moderate increase of O level were noted at the superficial layer (**d**). In the table, '−', '+', '++', and '+++' indicate none, slight, moderate, and high increase of each element, respectively. *C* non-treated control cementum, *US* ultrasonic scaler, *Er:YAG* Er:YAG laser, *CO_2* CO_2 laser

clearly demonstrated. The surface layer showed highly damaged microfragmentation with propagation of microcracks and microfissures, which incurred structural degradation as well as thermal denaturation, whereas the subsurface layer showed a dark staining possibly induced by only thermal change of the components. The highly damaged, fragile structure of the surface layer is considered to be undergoing ablation (ablating layer) [23].

In addition, in previous studies, the thickness of the affected layer was reported to be approximately 5 μm [16, 24], whereas in the present study, the layer was much thicker (approximately 20 μm) in the histological analysis. Considering the basic evidence that the surface layer of Er:YAG-lased cementum contains less organic components [25] and may be structurally fragile [24], it is speculated that most of the original surface microstructure of the treated surface was lost during the decalcification process in specimen preparation. Indeed, the thickness (mean 21.1 μm) of the affected layer in the present study coincides with that (mean 21.9 μm) observed following Er:YAG laser bone ablation by Sasaki et al. [26], who employed non-decalcified polished sections. Thus, non-decalcified thin sections would be suitable for precise analysis of the lased hard tissue surfaces.

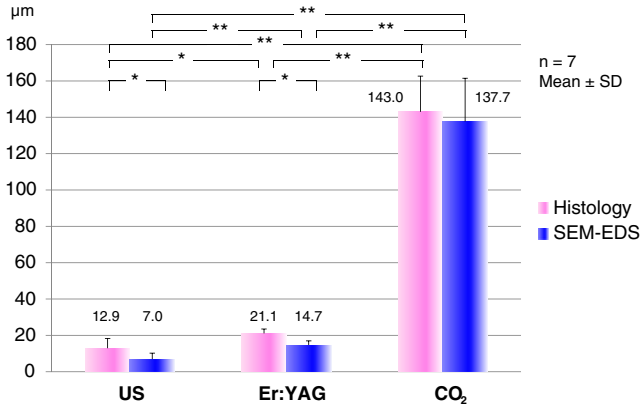

Fig. 5 Thickness of the affected layer in the histological analysis and SEM-EDS analysis. The thickness of the affected layer of the treated surface was determined from the zone of staining in the histological analysis and the zone showing the change of Ca and P levels as well as the change in the difference of both levels in SEM-EDS analysis. The thickness of the affected layer produced by CO_2 laser (CO_2) was markedly higher than those of the Er:YAG laser (*Er:YAG*) and the ultrasonic scaler (*US*). Statistically, the thickness of affected layer in the three different treatments was significantly different in each assessment ($p<0.01$). *$p<0.05$, **$p<0.01$. *US* ultrasonic scaler, *Er:YAG* Er:YAG laser, *CO_2* CO_2 laser

As for CO_2 laser treatment, CO_2-lased cementum has been previously reported to show only major thermal changes such as carbonization and microcracks [25, 27, 28]; however, in the present study, more interesting findings were observed.

Theoretically, the CO_2 laser is highly absorbed by water; however, the CO_2 laser is even more highly absorbed by the main mineral components of dental hard tissue, especially phosphate ions ($-PO_4$) in the carbonated hydroxyapatite [29, 30]. Therefore, the CO_2 laser energy applied to the hard tissue would be readily absorbed by the mineral components and thereby would cause instantaneous heat accumulation in the hard tissue, resulting in carbonization and vaporization of organic components and melting of the inorganic ones [6, 30, 31]. In the present study, the whitish product seen over the carbonization revealed by stereomicroscopy and the transparent product observed on the surface layer over the carbonization in the histological analysis would be the melted and resolidified inorganic components following complete vaporization of organic components. Actually, the melted and resolidified products were observed in the SEM analysis, resulting in marked increase of Ca and P levels in the superficial layer in SEM-EDS. In addition, in the histological analysis, the area of alteration induced by CO_2 laser could be divided into multiple differently structured/stained layers. These different layers may be associated with the various denatured products induced according to the gradient of severe temperature rise. In the CO_2-lased enamel and dentin, production of various types of calcium phosphates has been confirmed [32–34].

Regarding the Er:YAG-lased cementum, histological analysis revealed the fragility of the superficial layer. Maruyama et al. [24] reported that the surface microstructure of the lased cementum can be easily removed even by polishing with cotton pellets. Mizutani et al. [35] observed detachment of the newly formed cementum from the remaining cementum affected by Er:YAG laser in decalcified histological sections. Therefore, there is a concern regarding the longevity of periodontal tissue attachment to such fragile microstructures. However, clinically, Schwarz et al. [36, 37] demonstrated that the results of root debridement with the Er:YAG laser in periodontal pocket treatment were stable and maintained for 2 years, and that additional SRP on the laser-treated root surface seems to be unnecessary following laser therapy. These results suggest that the Er:YAG laser-treated root surface has clinically no negative influence on the wound healing of periodontal pockets. On the other hand, recently, better fibrin entrapment and/or blood clot adhesion on the microstructured bone surface following Er:YAG laser irradiation [26, 38] and better cell attachment to the Er:YAG-lased root surface than the mechanically treated one have been demonstrated [39, 40]. These findings indicate the advantageous effect of the Er:YAG-lased surface in initial wound healing. Moreover, unlike the CO_2 lased surface, no new toxic products were detected on the cementum surface irradiated by Er:YAG laser used under water cooling [25].

Comparing the thickness of altered cementum, the thickness after Er:YAG laser irradiation was markedly less than that obtained after CO_2 laser irradiation and was higher than that of the ultrasonic scaler. With the ultrasonic scaler, minimal alteration was detected due to heat production by friction [41]. Also, basically, the thickness determined by the change of Ca and P levels was smaller than that of the stained region in the histological analysis.

With SEM-EDS line micro-analysis, marked and slight increases of Ca and P were observed in the superficial layer of CO_2- and Er:YAG-lased cementum, respectively. Considering the evidence that decrease of organic components was detected on the Er:YAG- and CO_2-lased cementum [25], these findings could be attributed to the reduction of organic components following laser irradiation.

In the laser-affected layer except for the superficial layer of CO_2-lased tissue, basically the Ca and P levels were almost equal; in other words, the Ca/P ratio decreased compared to the deeper intact site in which Ca level was always higher than P. This may reflect the new products showing lower Ca/P ratio. For example, the formation of calcium pyrophosphate ($Ca_2P_2O_7$; Ca/P ratio = 1) occurs at temperatures of 200–600 °C [33, 42]. In fact, calcium pyrophosphates were identified as one of the various newly produced types of calcium phosphates on the Er:YAG-lased enamel [43].

In clinical practice, the CO_2 laser system is very efficient and widely used for soft tissue management. However, this laser readily produces severe thermal changes on the root surface. Thus, inadvertent focused CO_2 laser irradiation to the root surface must be prevented during gingival management [8, 22]. Compared to the CO_2 laser, the alteration of Er:YAG-lased cementum is minimal; however, further detailed investigations are required to evaluate the cementum alteration with the Er:YAG laser in clinical conditions as well as the effects of the microstructure of the lased surface in wound healing in vivo.

Conclusion

Er:YAG laser irradiation used with water cooling resulted in minimal cementum ablation and thermal changes with characteristic microstructure and degradation of the superficial layer. In contrast, CO_2 laser irradiation produced deep zones of severe thermal damage with distinct multiple affected layers accompanied by melted and resolidified structures and carbonization.

Acknowledgements This study was supported in part by a grant from the Global Center of Excellence (GCOE) Program of the International Research Center for Molecular Science in Tooth and Bone Diseases at Tokyo Medical and Dental University, and by a grant-in-aid for Scientific Research (C) (no. 22592308) to A.A., from the Ministry of Education, Culture, Sports, Science and Technology of Japan. The authors thank Drs. Makoto Kurosawa and Asuka Katagiri, Kurosawa Dental Clinic in Kumagaya, Saitama, Japan, for their valuable support.

References

1. Socransky SS, Haffajee AD (1992) The bacterial etiology of destructive periodontal disease: current concepts. J Periodontol 63:322–331
2. Kinane DF (2001) Causation and pathogenesis of periodontal disease. Periodontol 2000 25:8–20
3. Cobb CM (2002) Clinical significance of non-surgical periodontal therapy: an evidence-based perspective of scaling and root planing. J Clin Periodontol 29(Suppl 2):6–16
4. Oda S, Nitta H, Setoguchi T, Izumi Y, Ishikawa I (2004) Current concepts and advances in manual and power-driven instrumentation. Periodontol 2000 36:45–58
5. Adriaens PA, Edwards CA, De Boever JA, Loesche WJ (1988) Ultrastructural observations on bacterial invasion in cementum and radicular dentin of periodontally diseased human teeth. J Periodontol 59:493–503
6. Aoki A, Sasaki K, Watanabe H, Ishikawa I (2004) Lasers in nonsurgical periodontal therapy. Periodontol 2000 36:59–97
7. Ishikawa I, Aoki A, Takasaki AA, Mizutani K, Sasaki KM, Izumi Y (2009) Application of lasers in periodontics: true innovation or myth? Periodontol 2000 50:90–126
8. Pick RM, Colvard MD (1993) Current status of lasers in soft tissue dental surgery. J Periodontol 64:589–602
9. Hibst R, Keller U (1989) Experimental studies of the application of the Er:YAG laser on dental hard substances: I. Measurement of the ablation rate. Lasers Surg Med 9:338–344
10. Keller U, Hibst R (1989) Experimental studies of the application of the Er:YAG laser on dental hard substances: II. Light microscopic and SEM investigations. Lasers Surg Med 9:345–351
11. Kayano T, Ochiai S, Kiyono K, Yamamoto H, Nakajima S, Mochizuki T (1991) Effect of Er:YAG laser irradiation on human extracted teeth. J Clin Laser Med Surg 9:147–150
12. Hale GM, Querry MR (1973) Optical constants of water in the 200-nm to 200-μm wavelength region. Appl Opt 12:555–563
13. Watanabe H, Ishikawa I, Suzuki M, Hasegawa K (1996) Clinical assessments of the erbium:YAG laser for soft tissue surgery and scaling. J Clin Laser Med Surg 14:67–75
14. Schwarz F, Sculean A, Georg T, Reich E (2001) Periodontal treatment with an Er:YAG laser compared to scaling and root planing. A controlled clinical study. J Periodontol 72:361–367
15. Aoki A, Ando Y, Watanabe H, Ishikawa I (1994) In vitro studies on laser scaling of subgingival calculus with an erbium:YAG laser. J Periodontol 65:1097–1106
16. Aoki A, Miura M, Akiyama F, Nakagawa N, Tanaka J, Oda S, Watanabe H, Ishikawa I (2000) In vitro evaluation of Er:YAG laser scaling of subgingival calculus in comparison with ultrasonic scaling. J Periodontol Res 35:266–277
17. Schwarz F, Putz N, Georg T, Reich E (2001) Effect of an Er:YAG laser on periodontally involved root surfaces: an in vivo and in vitro SEM comparison. Lasers Surg Med 29:328–335
18. Schwarz F, Sculean A, Berakdar M, Szathmari L, Georg T, Becker J (2003) In vivo and in vitro effects of an Er:YAG laser, a GaAlAs diode laser, and scaling and root planing on periodontally diseased root surfaces: a comparative histologic study. Lasers Surg Med 32:359–366
19. Eberhard J, Ehlers H, Falk W, Acil Y, Albers HK, Jepsen S (2003) Efficacy of subgingival calculus removal with Er:YAG laser compared to mechanical debridement: an in situ study. J Clin Periodontol 30:511–518
20. Schwarz F, Aoki A, Becker J, Sculean A (2008) Laser application in non-surgical periodontal therapy: a systematic review. J Clin Periodontol 35:29–44
21. Gaspirc B, Skaleric U (2007) Clinical evaluation of periodontal surgical treatment with an Er:YAG laser: 5-year results. J Periodontol 78:1864–1871
22. The Research, Science and Therapy Committee of the American Academy of Periodontology (2002) Lasers in periodontics (Academy report), authored by Cohen RE and Ammons WF, revised by Rossman JA. J Periodontol 73:1231–1239
23. Aoki A, Ishikawa I, Yamada T, Otsuki M, Watanabe H, Tagami J, Ando Y, Yamamoto H (1998) Comparison between Er:YAG laser and conventional technique for root caries treatment in vitro. J Dent Res 77:1404–1414
24. Maruyama H, Aoki A, Sasaki KM, Takasaki AA, Iwasaki K, Ichinose S, Oda S, Ishikawa I, Izumi Y (2008) The effect of chemical and/or mechanical conditioning on the Er:YAG laser-treated root cementum: analysis of surface morphology and periodontal ligament fibroblast attachment. Lasers Surg Med 40:211–222
25. Sasaki KM, Aoki A, Masuno H, Ichinose S, Yamada S, Ishikawa I (2002) Compositional analysis of root cementum and dentin after Er:YAG laser irradiation compared with CO_2 lased and intact roots using Fourier transformed infrared spectroscopy. J Periodontol Res 37:50–59
26. Sasaki KM, Aoki A, Ichinose S, Ishikawa I (2002) Ultrastructural analysis of bone tissue irradiated by Er:YAG laser. Lasers Surg Med 31:322–332

27. Israel M, Cobb CM, Rossmann JA, Spencer P (1997) The effects of CO_2, Nd:YAG and Er:YAG lasers with and without surface coolant on tooth root surfaces. An in vitro study. J Clin Periodontol 24:595–602
28. Sasaki KM, Aoki A, Ichinose S, Ishikawa I (2002) Morphological analysis of cementum and root dentin after Er:YAG laser irradiation. Lasers Surg Med 31:79–85
29. Featherstone JDB (2000) Caries detection and prevention with laser energy. Dent Clin North Am 44:955–969
30. Fried D, Zuerlein M, Featherstone JDB, Seka W, McCormack SM (1997) IR laser ablation of dental enamel: mechanistic dependence on the primary absorber. Appl Surf Sci 127:852–856
31. Seka W, Featherstone JDB, Fried D, Visuri SR, Walsh JT (1996) Laser ablation of dental hard tissue: from explosive ablation to plasma-mediated ablation. Proc SPIE 2672:144–158
32. Kuroda S, Fowler BO (1984) Compositional, structural, and phase changes in in vitro laser-irradiated human tooth enamel. Calcif Tissue Int 36:361–369
33. Fowler BO, Kuroda S (1986) Changes in heated and in laser-irradiated human tooth enamel and their probable effects on solubility. Calcif Tissue Int 38:197–208
34. Rohanizadeh R, LeGeros RZ, Fan D, Jean A, Daculsi G (1999) Ultrastructural properties of laser-irradiated and heat-treated dentin. J Dent Res 78:1829–1835
35. Mizutani K, Aoki A, Takasaki AA, Kinoshita A, Hayashi C, Oda S, Ishikawa I (2006) Periodontal tissue healing following flap surgery using an Er:YAG laser in dogs. Lasers Surg Med 38:314–324
36. Schwarz F, Sculean A, Berakdar M, Georg T, Reich E, Becker J (2003) Periodontal treatment with an Er:YAG laser or scaling and root planing. A 2-year follow-up split-mouth study. J Periodontol 74:590–596
37. Schwarz F, Sculean A, Berakdar M, Georg T, Reich E, Becker J (2003) Clinical evaluation of an Er:YAG laser combined with scaling and root planing for non-surgical periodontal treatment. A controlled, prospective clinical study. J Clin Periodontol 30:26–34
38. Pourzarandian A, Watanabe H, Aoki A, Ichinose S, Sasaki K, Nitta H, Ishikawa I (2004) Histological and TEM examination of early stages of bone healing after Er:YAG laser irradiation. Photomed Laser Surg 22:355–363
39. Schwarz F, Aoki A, Sculean A, Georg T, Scherbaum W, Becker J (2003) In vivo effects of an Er:YAG laser, an ultrasonic system and scaling and root planing on the biocompatibility of periodontally diseased root surfaces in cultures of human PDL fibroblasts. Lasers Surg Med 33:140–147
40. Belal MH, Watanabe H, Ichinose S, Ishikawa I (2007) Effect of Er:YAG laser combined with rhPDGF-BB on attachment of cultured fibroblasts to periodontally involved root surfaces. J Periodontol 78:1329–1341
41. Nicoll BK, Peters RJ (1998) Heat generation during ultrasonic instrumentation of dentin as affected by different irrigation methods. J Periodontol 69:884–888
42. LeGeros RZ (1975) The unit-cell dimensions of human enamel apatite: effect of chloride incorporation. Arch Oral Biol 20:63–71
43. Eguro T (1998) Structural and compositional changes of human enamel by the Er:YAG laser irradiation. J Jpn Conserv Dent 41:582–595